Catalysis Today 175 (2011) 328–337

Contents lists available at ScienceDirect

Catalysis Today

journal homepage: www.elsevier.com/locate/cattod

Pt-MgZnCuAl hydrotalcite-derived catalysts in the reduction of nitrates using continuous and batch reactors

N. Barrabés[a,*], M.A. Garrido[b], A. Frare[a], A. Monzón[b], D. Tichit[a]

[a] Equipe MACS, Institut Charles Gerhardt UMR 5253 CNRS/UM2/ENSCM/UM1, Matériaux AVancés pour la Catalyse et la Santé, 8 rue Ecole Normale, 34296 Montpellier Cedex 5, France
[b] Institute of Nanoscience of Aragon, Department of Chemical and Environmental Engineering, University of Zaragoza, C/Mariano Esquillor s/n, 50018, Zaragoza, Spain

ARTICLE INFO

Article history:
Received 15 October 2010
Received in revised form 3 February 2011
Accepted 30 March 2011
Available online 15 June 2011

Keywords:
Nitrate removal
Hydrotalcite
Acidity
Reconstruction
Batch reactor
Continuous reactor

ABSTRACT

The role of acid–base properties and reconstruction degree of the hydrotalcite-derived materials (MgZnCuAl) in the catalytic hydrogenation of nitrates reaction is studied. In addition, the catalysts have been tested in a batch and continuous reactor to evaluate the influence of the reactor configuration on the catalytic performance. The characterizations of the samples have been performed by XRD, TPR, BET, TEM and MBOH test reaction. A clearly influence of the acid–base properties of the catalysts, modulated by the Zn incorporation, is observed with an increase in the nitrogen selectivity. Besides the common operational parameter differences between work in continuous and discontinuous systems, it shows great differences in the reconstruction degree of the samples. Higher reconstruction leads to higher nitrate reduction and a decrease of nitrite production.

1. Introduction

Wastewater treatment has become a social, technological, economical and political problem. Diffuse pollution of water resources from agricultural sources particularly the increase in the nitrate concentration in ground and surface water is a major environmental issue. The nitrate anions are proven to be harmful to the mammalian organisms where they are transformed to ammonium. An intermediate step is the partial reduction of nitrate to nitrite. The nitrite can cause a blue baby syndrome and it is also a precursor to the carcinogenic nitrous amine. European studies recommend a maximum nitrate (NO_3^-) concentration of 10 mg/l, nitrite (NO_2^-) of 0.03 mg/l and ammonium (NH_4^+) of 0.4 mg/l in drinking water. Whereas the legal limits imposed within the EU are 50, 0.1 and 0.5 ppm for NO_3^-, NO_2^- and NH_4^+, respectively.

Many of physicochemical and biological processes have been developed for removing nitrate from contaminated water, yet these processes might be either marginally cost-effective or detrimental due to potential side-effect on water quality. Catalytic denitrification is emerging as the most promising and flexible technique. In this process, nitrate ions are reduced using hydrogen over bimetallic catalyst. It follows a consecutive reaction scheme with nitrite as intermediate and nitrogen and ammonia as final products [1]. One of the advantages of the catalytic reduction of nitrate containing effluents is that the reaction is performed in mild conditions, room temperature and atmospheric pressure [2–5].

Bimetallic platinum or palladium based supported catalysts have been extensively studied for this reaction [6–12]. The mechanism generally admitted is that nitrates are reduced to nitrites on metallic copper which is oxidized according to a redox reaction. The noble metal activates the hydrogen and then enables copper reduction. A wide variety of supports have been investigated such as γ-Al_2O_3, silica, active carbon, glass fiber, pumice, bacterial cellulose nanofibers, TiO_2 for example. Hydrotalcites (HTs) have been recently shown as suitable precursors of catalysts for this reaction.

Palomares et al. [13] used Pd-Cu/Mg/Al catalysts obtained by impregnation of the noble metal on Cu/Mg/Al mixed oxide obtained by calcination of a Cu/Mg/Al LDH. It led to a more active and selective catalyst than $PdCu/Al_2O_3$. The high activity was related to the specific property of the mixed oxides supports obtained by calcination of the HTs to be reconstructed in the lamellar form with nitrate anions intercalated between the layers. On the other hand, the good selectivity, due to the low ammonia formation, was assigned to a decrease of the diffusion limitations. Several methods are available to prepare metal supported catalysts from HTs.

Wang and co-workers [14] reported higher adsorption and catalytic activity for the samples obtained by co-precipitation rather

* Corresponding author. Present address: Institute of Materials Chemistry, Vienna University of Technology, Getreidemarkt 9/BC/01, A-1060 Vienna, Austria.
Tel.: +43 1 58801x165125/33 0 4 67 16 34 77;
fax: +43 1 58801x165980/33 0 4 67 16 34 70.
E-mail address: noe.barrabes@gmail.com (N. Barrabés).

0920-5861/$ – see front matter © 2011 Elsevier B.V. All rights reserved.
doi:10.1016/j.cattod.2011.03.063

than by co-impregnation. High selectivity was also reached and related with a pH buffering capacity of the hydrotalcite when hydroxyls are released during the reconstruction of the mixed oxide into hydrotalcite [15]. The control in the ammonia formation by a pH buffering from the support has been also demonstrated recently by Barrabes et al. [16] with $Pt/CeFO_2$ catalysts obtained by combustion. It was shown that an acidity increase of the support leads to a decrease in the ammonia formation, increasing the selectivity of the process to nitrogen.

Pd and Pt show different behaviour depending on the support. Nevertheless, in the previous works with hydrotalcite-like catalysts Pd was mainly employed in an amount ranging from 1 to 5 wt%, taking in account future application in large scale, the amount of noble metal should be optimized, due to the high economical value. Nevertheless, to our knowledge, comparison with Pt-containing hydrotalcite-like catalysts has not been performed. Therefore an interesting goal was to investigate the properties of the platinum based supported catalysts obtained from hydrotalcite precursors.

Beside several studies showed that the selectivity toward ammonia is governed by the intermediate nitrite hydrogenation describing a structure-sensitive process. Yoshinaga et al. [17] reported that the formation of ammonia depend on the coordination of the Pd atoms. Epron et al. [3] and Sá et al. [18], showed that an active bimetallic site requires a close proximity between the two metals and that formation of an alloy is not required. In such case the hydrogen activated on the noble metal sites migrates by spill-over to the copper sites [19].

In order to contemplate the main parameters affecting the activity and selectivity of supported bimetallic catalysts obtained from hydrotalcite-like precursors in the nitrates reduction, multicationic MgZnCuAl HTs have been used as precursors of mixed oxides then impregnated with Pt. This composition was chosen first to take advantage of the adsorptive properties of the HT structure during reconstruction which is the highest in the Mg- and Al-containing materials. Second, Cu was introduced by co-precipitation because it leads to small and well dispersed particles. Third, in order to benefit of the buffering by the support several amounts of Zn have been also introduced in the HT structure with the aim to modulate the acid–base properties. Lastly two different Pt impregnation protocols have been followed, looking for different Pt sites on the surface. These materials have been characterized by several techniques as TPR, XRD, BET and TEM, in order to correlate the physicochemical properties of the catalysts with the activities and selectivity in the nitrate reduction.

2. Experimental

2.1. Preparation of catalysts

MgZnAl and MgZnCuAl HTs were prepared by co-precipitation at constant pH of an aqueous solution of $Mg(NO_3)_2{\cdot}6H_2O$, $Al(NO_3)_3{\cdot}9H_2O$, $Zn(NO_3)_2{\cdot}6H_2O$ (MgZnAl HT) (and $Cu(NO_3)_2{\cdot}5H_2O$ for MgZnCuAl HT) in adequate amounts, with a second solution of NaOH. Both solutions were simultaneously added at a control rate to a beaker containing distilled water under vigorous stirring, at a pH value around 9–10 and room temperature. The resulting suspension was then kept at 80 °C with further stirring for 18 h. The resulting solid was filtered, washed several times with distilled water and dried at 100 °C for 18 h. 4 MgZnCuAl HTs samples with (Mg + Zn + Cu)/Al molar ratio of 3 and Mg:Zn:Cu = 1.5:0.3:1.2; 0.5:1:1.5; 1:1:1; 1:0.5:1.5 and 1.5:1.4:0.1 were thus obtained and further noted $Mg_{1.5}Zn_{0.3}Cu_{1.2}Al_1$; $Mg_{0.5}Zn_1Cu_{1.5}Al_1$; $Mg_1Zn_1Cu_1Al_1$, $Mg_1Zn_{0.5}Cu_{1.5}Al_1$ and $Mg_{1.5}Zn_{1.4}Cu_{0.1}Al_1$, respectively. A MgZnAl HT with (Mg + Zn)/Al molar ratio of 3 and Mg:Zn = 1.5:1.5; 1:2 and 2:1 was noted $Mg_{1.5}Zn_{1.5}Al_1$, $Mg_2Zn_1Al_1$ and $Mg_1Zn_2Al_1$. Also MgAl HT with Mg/Al molar ratio of 2 was prepared.

The HTs samples were calcined at 500 °C for 4 h obtaining mixed oxides hereafter noted $Mg_{1.5}Zn_{0.3}Cu_{1.2}Al_1O$; $Mg_{0.5}Zn_1Cu_{1.5}Al_1O$; $Mg_1Zn_1Cu_1Al_1O$; $Mg_{1.5}Zn_{1.4}Cu_{0.1}Al_1O$ and $Mg_{1.5}Zn_{1.5}Al_1O$. For the impregnation of the noble metals (Pt) on the $Mg_xZn_yCu_zAl_1O$ mixed oxide two different protocols were applied: in the first protocol (labelled as CRPt) the $Mg_xZn_yCu_zAl_1O$ mixed oxide was reduced under hydrogen for 2 h at 400 °C. The reduced $Cu^0Mg_xZn_yAl_1O$ sample was then introduced into an ethanol solution containing the required amount of platinum salt (K_2PtCl_6), corresponding to the 0.5 wt%, under stirring at room temperature. All steps were carried out under argon atmosphere in order to avoid reoxidation of copper. The noble metal solution had been degassed by bubbling with argon for 1 h before adding the reduced Cu-containing mixed oxide. In this step Pt is reduced by a redox process with copper. Then the solid was filtered and dried at 100 °C. Finally, calcination was performed for 2 h at 300 °C. A new reduction process was carried out in a hydrogen flow of 7 ml/min for 60 min at 350 °C prior to the reaction. In the second protocol (labelled as CPt), the reduction step of copper before the Pt introduction was not performed. The $Mg_xZn_yCu_zAl_1O$ mixed oxide was impregnated with an ethanol solution of K_2PtCl_6. Then the solid was dried at 100 °C, followed by calcination and reduction as in the first protocol. Samples were also prepared by co-impregnated of Mg_xZn_yAlO mixed oxides by an ethanol solution containing the required amounts of Pt (K_2PtCl_6) and Cu ($Cu(NO_3)_2{\cdot}5H_2O$) salts to obtain 0.5 wt% Pt and 2 wt% Cu in the sample. Then the material was dry overnight at 100 °C and calcined at 300 °C for 2 h obtaining the catalyst.

2.2. Catalysts characterization

Powder X-ray diffraction (XRD) patterns of the different samples were obtained on a Siemens D5000 diffractometer using (40 kV, 20 mA) using monochromatized Cu Kα radiation (λ = 1.541 Å) and a scan rate of 1 K min^{-1}. The patterns were recorded over a range of 2θ angles from 5° to 70° and crystalline phases were identified using the Joint Committee on Powder Diffraction Standards (JCPDS) files.

BET surface area was calculated from N_2 adsorption–desorption isotherms for calcined samples. The physisorption was performed on Micromeritics ASAP 2000 surface analyzer at 77 K. Before analysis, all the samples were degassed in vacuum at 393 K for 6 h.

FTIR spectra were taken on a Compact Fourier transform infrared spectrophotometer. IRAffinity-1 Shimadzu with a S/N ratio of (30,000:1, 1-min accumulation, neighborhood of 2100 cm^{-1}, peak-to-peak), a maximum resolution of 0.5 cm^{-1}.

Transmission electron micrographs were taken of the samples using a JEOL-2010 electronic microscope operating at an accelerating voltage of 200 kV. Samples for TEM were prepared by depositing the sample on the copper grid and then the solvent was allowed to evaporate under vacuum before analysis.

Temperature-programmed reduction (TPR) studies of the samples were performed using a TPD/R/O 1100 (ThermoFinnigan) equipped with a thermal conductivity detector (TCD) and coupled to a mass spectrometer QMS 422 Omnistar. Before reduction, the sample (around 100 mg) was dried under flowing helium at 120 °C for 24 h. The reduction was carried out between room temperature and 900 °C at a heating rate of 10 °C/min flowing a gas mixture of 5% H_2 in argon (20 ml/min total flow).

The conversion of 2-methyl-3-butyn-2-ol MBOH was studied as catalytic test reaction for the characterization of the acido-basic properties of the materials. The conversion of MBOH was performed under atmospheric pressure at 140 °C in a micro flow fixed-bed reactor using 200 mg of the calcined samples. MBOH was fed by bubbling N_2 through a saturator at 25 °C (P_{MBOH} = 2.51 kPa).

Analysis of MBOH as the products has been performed by gas chromatography (Hewlett Packard Model 5890) using Megabor capillary column (30 m × 0.546 mm) and FID detection.

2.3. Catalytic activity

2.3.1. Continuous reactor system

A simplified diagram of the experimental setting is shown and explained in previous work [12]. The reactor was filled with 0.5 g of catalyst. The catalytic reduction of nitrate was performed in a fixed-bed reactor. The liquid feed solution with 60 mg/l of nitrate ions was introduced by a pump (70 ml/h). The hydrogen flow is adjusted by a mass flow controller (3 ml/min) and the catalytic system worked at ambient temperature and pressure. The reaction products were analyzed by the HPLC coupled with conductivity detector (Shimatzu). Nitrate and nitrite concentration were determined after separation on a Shim-pack IC-A1S column at 40 °C. Ammonium ions were quantified using a Shodex IC YK-421 column at 40 °C.

2.3.2. Semi-batch reactor system

Catalytic reduction of nitrates was carried out also in a semi-batch reactor. The catalysts were tested in a 1-L glass reactor equipped with a magnetic stirrer, pH and temperature control, selective electrodes for the reactants and products quantification (NO_3^-, NO_2^- and NH_4^+) and a septum for sampling. Gases (H_2 and N_2) were fluxed into the vessel through a bubbler and the flow was adjusted by electronic mass flow controller. Normally, the reactor is filled with 0.6 L of distilled water (7.7 μS/cm) and purged with nitrogen for 30 min. Then, in a typical run, 0.5 g of the powder catalyst previously reduced with hydrogen at 300 °C is charged into the reactor purged with hydrogen for 15 min. The reaction starts with the addition of 25 cm^3 of a 2500 ppm $NaNO_3$ solution (Panreac, 99%), in order to achieve a total nitrate concentration of 100 mg/l in the liquid. During the reaction a hydrogen flow of 450 cm^3/min was introduced in the reactor. The experiments were carried out at 25 °C, and the reactor was stirred at 950 rpm. The reaction progress was followed by taking, at defined periods, small aliquots (10 cm^3) for the determination of nitrate, nitrite and ammonia concentration by UV–vis spectroscopy (Hach Lange spectrophotometer, model DR 2800) combined with colorimetric kits at λ = 345 nm, 515 and 690 nm, respectively. Detection limits of nitrate, nitrite and ammonium were 1–155, 0.005–20.0 and 0.015–60.0 ppm, respectively.

3. Results

3.1. Characterization results

3.1.1. Fresh materials

The XRD patterns of the as-prepared and calcined HT samples are displayed in Figs. 1 and 2, respectively. They are characteristic of the hydrotalcite structure with particularly peaks at $2\theta = 10.5°$ and 21° corresponding to the reflections on the (0 0 3) and (0 0 6) crystal planes which allow to calculate a d_{003} basal spacing of 0.84 nm in agreement with the presence of nitrate as main compensating anions, and (1 1 0) peaks at $\sim 2\theta = 61°$ (Fig. 1). Segregation of oxide copper, i.e. tenorite phase is clearly detected in all the $Mg_xZn_yCu_zAl_1$ HT samples, denoted by the diffraction peaks at 35.5° and 38° 2θ whose intensities increase with Cu molar fraction in the syntheses solutions. Multicationic HTs often exhibit low crystallinity owing to distortions of the layers when cations of different ionic sizes are combined. Regarding the $Mg_xZn_yCu_zAl_1$ HTs of this study, it is worthy to note that crystallinity increases when Zn molar fraction increases. This is in agreement with the higher crystallinity of Zn/Al HTs than Mg/Al HTs generally observed [20], so as Cu mainly segregates as CuO. $Mg_{1.5}Zn_{1.5}Al_1$ is poorly crystalline

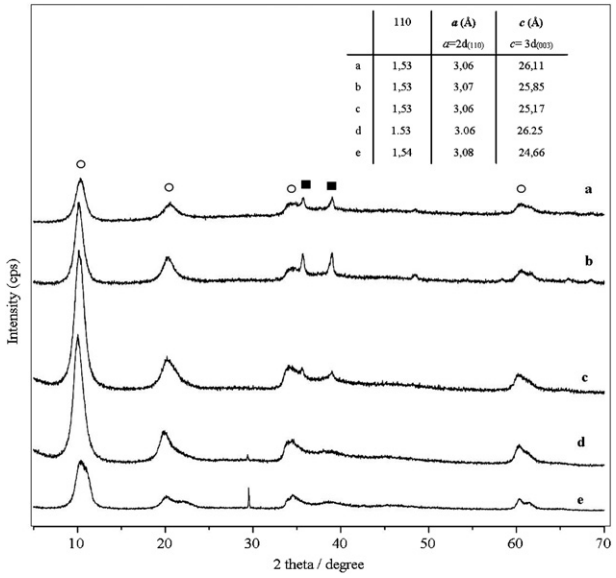

Fig. 1. XRD profiles of: (a) $Mg_{1.5}Zn_{0.3}Cu_{1.2}Al_1$; (b) $Mg_{0.5}Zn_1Cu_{1.5}Al_1$; (c) $Mg_1Zn_1Cu_1Al_1$; (d) $Mg_{1.5}Zn_{1.4}Cu_{0.1}Al_1$ and (e) $Mg_{1.5}Zn_{1.5}Al_1$ samples. (○) Hydrotalcite phase; (■) CuO phase.

and the broadening of the (0 0 1) peaks suggests the formation of a mixture of Mg/Al and Zn/Al HTs rather than an $Mg_xZn_yAl_1$ HT.

The XRD patterns of the samples calcined at 500 °C (Fig. 2) show the presence of Mg(Al)O, CuO and ZnO crystalline phases whose respective amount obviously depend on the cationic composition of the precursors HTs. Indeed the most intense reflections are due to the well crystallized ZnO phase in $Mg_{1.5}Zn_{1.4}Cu_{0.1}Al_1O$ and $Mg_{1.5}Zn_{1.5}Al_1O$ and to the tenorite CuO phase in $Mg_{1.5}Zn_{0.3}Cu_{1.2}Al_1O$ and $Mg_{0.5}Zn_1Cu_{1.5}Al_1O$. Both phases give peaks of similar intensities in $Mg_1Zn_1Cu_1Al_1O$ in agreement with its composition. The Mg(Al)O mixed oxide phase gives in contrast weak and broad reflections at $2\theta = 43°$ and 62.5° detected in $Mg_1Zn_1Cu_1Al_1O$, $Mg_{1.5}Zn_{1.4}Cu_{0.1}Al_1O$ and $Mg_{1.5}Zn_{1.5}Al_1O$ samples (Fig. 2). These results suggest that both ZnO and CuO phases formed

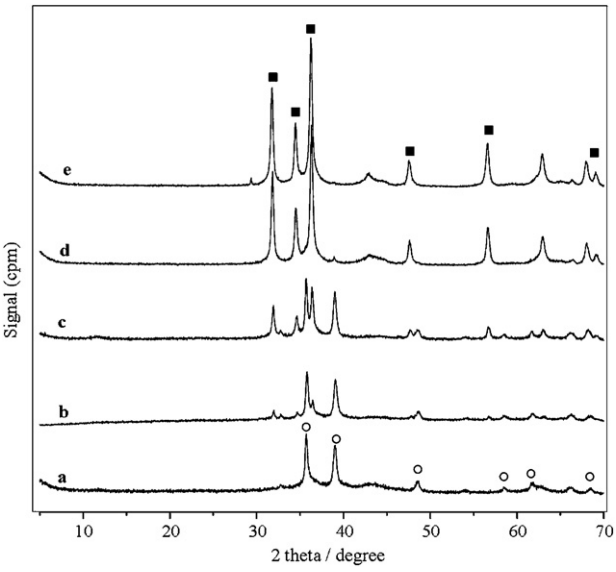

Fig. 2. XRD profiles of: (a) $Mg_{1.5}Zn_{0.3}Cu_{1.2}Al_1O$; (b) $Mg_{0.5}Zn_1Cu_{1.5}Al_1O$; (c) $Mg_1Zn_1Cu_1Al_1O$; (d) $Mg_{1.5}Zn_{1.4}Cu_{0.1}Al_1O$ and (e) $Mg_{1.5}Zn_{1.5}Al_1O$ samples. (■) ZnO phase; (○) CuO phase.

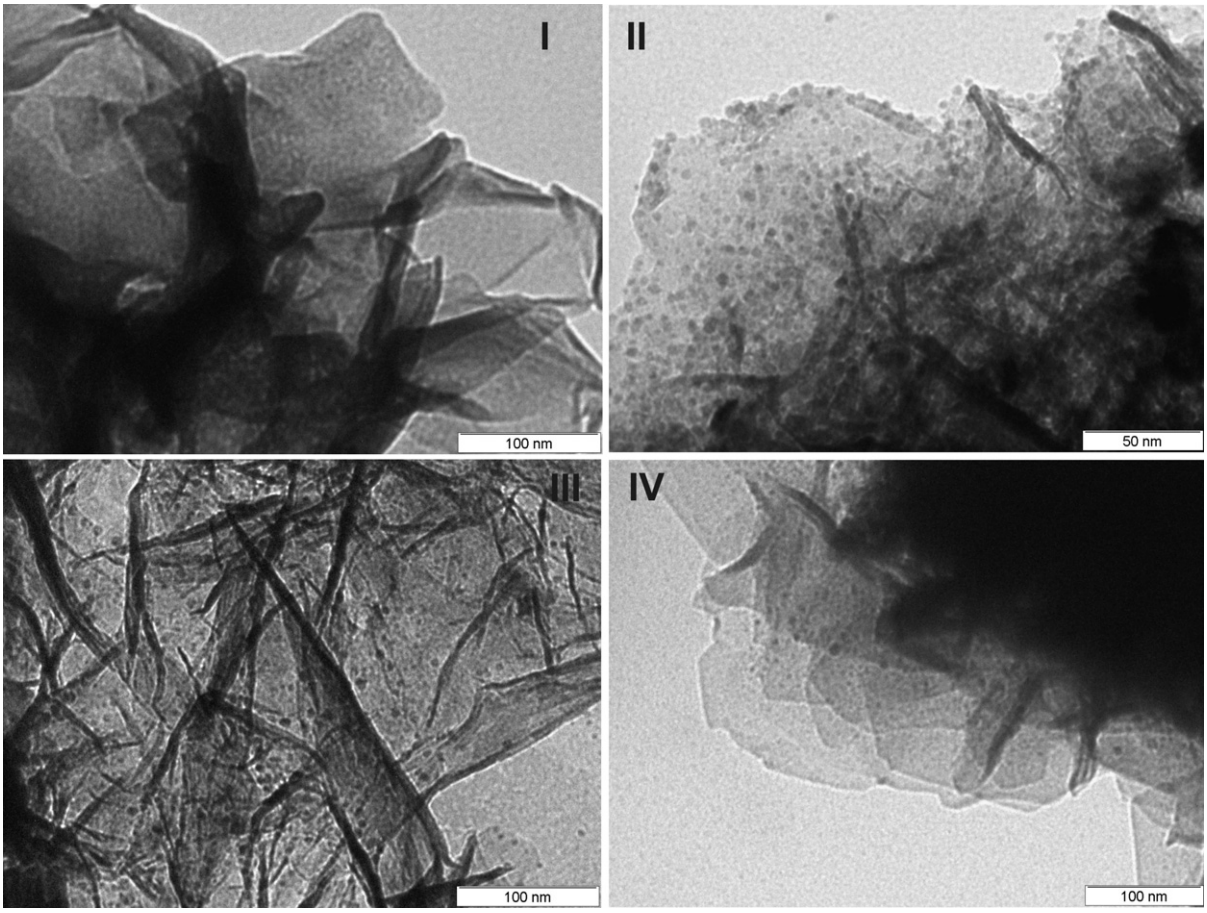

Fig. 3. TEM picture: (I) hydrotalcite; (II) calcined hydrotalcite; (III) CPt catalyst and (IV) CRPt catalyst.

well crystallized and dispersed particles on the Mg(Al)O matrix [21].

The XRD patterns of the different Pt-containing catalysts are similar to those of the mixed oxides previously described due to the low amount of Pt introduced (0.5 wt%).

TEM images of the precursor $Mg_1Zn_1Cu_1Al_1$ HTs, the $Mg_1Zn_1Cu_1Al_1O$ mixed oxide support and the catalysts representative of all samples are reported on Fig. 3. $Mg_1Zn_1Cu_1Al_1$ show the characteristic morphology of HT samples with particles of regular shape of ca. 100 nm in length. The layer structure can be distinguished in same of the aggregates (Fig. 3(I)). After calcination of the sample, two types of particles with different morphologies are clearly identified. Particles with a fibrous shape due to the topotactic decomposition of the HT to give mixed oxide, and granular spots of homogeneous size of ca. 5 nm are assignable to the segregated CuO phase. (Fig. 3(II)). No significant changes are observed for the Pt-containing samples prepared following the CPt and CRPt protocols (Fig. 3(III) and (IV)).

Nitrogen adsorption–desorption isotherms of the $Mg_xZn_yCu_zAl_1O$ mixed oxides are displayed in Fig. 4. All samples present type IV adsorption isotherm according to IUPAC classification which corresponds to mesoporous solids. In addition, hysteresis loops are type H3, indicating the presence of slit-shaped pores with non-uniform size and shape as generally found for calcined layered materials [22]. Specific surface areas in a similar range from 77 to 96 $m^2\ g^{-1}$ are not related to the cationic composition of the mixed oxides.

The acid–base properties of the mixed oxides have been investigated using the catalytic test reaction of conversion of 2-methyl-3-butyn-2-ol (MBOH). MBOH is converted on acid sites into 3-methyl-3-buten-1-yne (Mbyne) and 3-methyl-2-buten-1-al (Prenal), while on basic sites it undergoes decomposition into acetone and acetylene. Fig. 5 shows the catalytic activity in the conversion of MBOH of the $Mg_xZn_yCu_zAl_1O$ mixed oxides and, for sake of comparison, of Mg(Al)O. Acetone and acetylene produced in quantitative amounts are the only reaction products accounting for the presence in all samples of mainly basic sites. Mg(Al)O is as expected the most active catalyst. The activity increases when Mg content increases at the expense of Zn content in the $Mg_xZn_yCu_zAl_1O$ mixed oxides. This is in agreement with the well known higher basicity of MgO than ZnO single oxide.

The results of the TPR of the $Mg_xZn_yCu_zAl_1O$ mixed oxides are displayed in Fig. 6(I). All the samples present a broad reduction peak between 200 °C and 380 °C assigned to the reduction of CuO species. They are reduced at lower temperature than in the precursors HT samples (not shown) where reduction peaks were recorded between 300 °C and 400 °C. This fact could be related with the segregation of CuO phase during the calcination process. In this way, depending on the amount of CuO phase segregated the reduction temperature is slightly modified. Indeed for $Mg_{1.5}Zn_{0.3}Cu_{1.2}Al_1O$ and $Mg_{0.5}Zn_1Cu_{1.5}Al_1O$ with higher Cu content a broad peak is observed toward lower temperature which could be related to well disperse CuO particles easily reduced. In all samples the peak at higher temperature is assigned to sintered copper oxide particles or CuO interacting with the support or another metal.

TPR profiles of the 0.5% $PtMg_1Zn_{0.5}Cu_{1.5}Al_1O$ and 0.5% $PtMg_{1.5}Zn_{0.3}Cu_{1.2}Al_1O$ catalysts prepared following the two protocols (CPt and CRPt) for the introduction of Pt are shown in the Fig. 6(II). The TPR profiles of the samples prepared by the CPt protocol are similar to those of the Pt-free samples. The only change

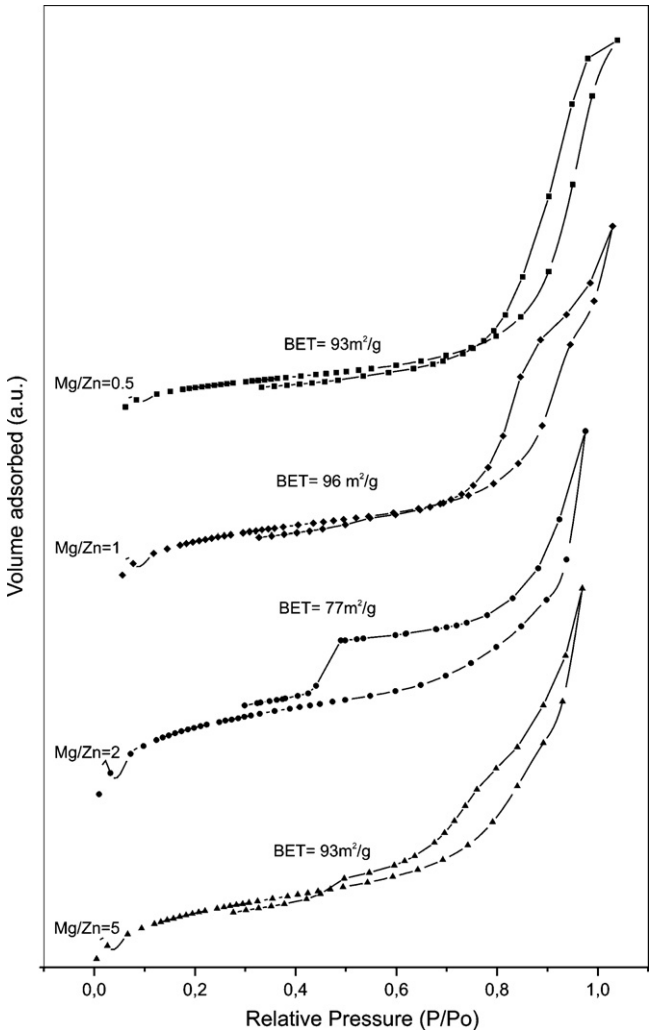

Fig. 4. Nitrogen adsorption–desorption isotherms of $Mg_{1.5}Zn_{0.3}Cu_{1.2}Al_1O$; $Mg_1Zn_1Cu_1Al_1O$ and $Mg_{0.5}Zn_1Cu_{1.5}Al_1O$ samples.

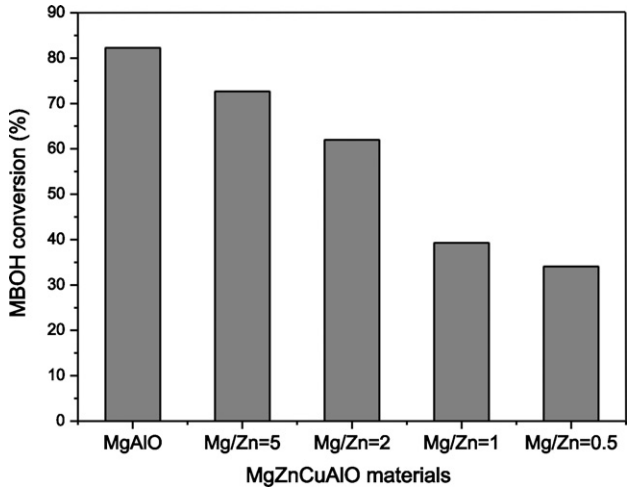

Fig. 5. Catalytic activity in the MBOH reaction of MgAlO, $Mg_{1.5}Zn_{0.3}Cu_{1.2}Al_1O$, $Mg_1Zn_{0.5}Cu_{1.5}Al_1O$, $Mg_1Zn_1Cu_1Al_1O$ and $Mg_{0.5}Zn_1Cu_{1.5}Al_1O$ samples.

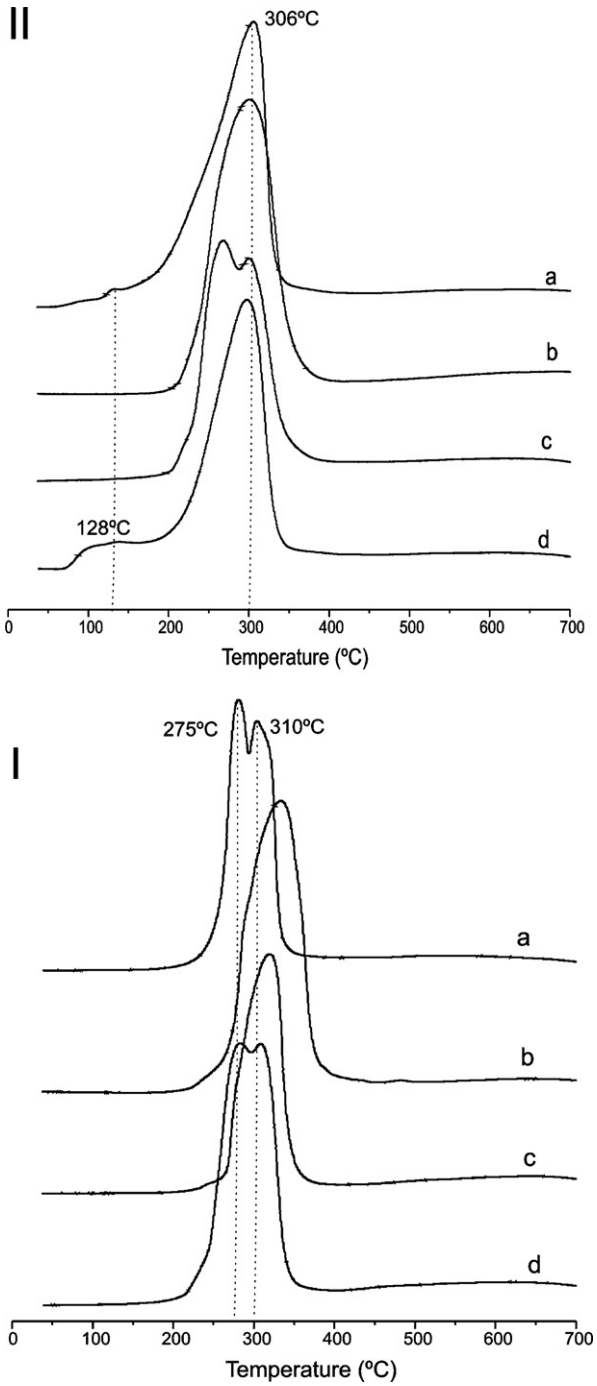

Fig. 6. TPR profiles of calcined hydrotalcites (I) [a: $Mg_{1.5}Zn_{0.3}Cu_{1.2}Al_1O$; b: $Mg_1Zn_{0.5}Cu_{1.5}Al_1O$; c: $Mg_1Zn_1Cu_1Al_1O$; d: $Mg_{0.5}Zn_1Cu_{1.5}Al_1O$] and catalysts by the CPt and CRPt protocols (II) [a: 0.5% $PtMg_1Zn_{0.5}Cu_{1.5}Al_1O$ CRPt; b: 0.5% $PtMg_1Zn_{0.5}Cu_{1.5}Al_1O$ CPt; c: 0.5% $PtMg_{1.5}Zn_{0.3}Cu_{1.2}Al_1O$ CPt; d: 0.5% $PtMg_{1.5}Zn_{0.3}Cu_{1.2}Al_1O$ CRPt].

is a shift of ca. 30 °C toward higher temperature of the reduction temperature in 0.5% Pt-$Mg_2Zn_1CuAl_1O$-CPt comparatively to $Mg_2Zn_1CuAl_1O$. In contrast, the reduction peak begins at lower temperature and is clearly split in two components for the samples prepared by the CRPt protocol showing that a larger amount of CuO species become more easily reduced. This behaviour could be related to a close contact between the metals rather than to a high interaction between Pt–Cu or to alloy formation [23].

In order to compare the effect of Cu protocol incorporation either by impregnation on the mixed oxide support or by

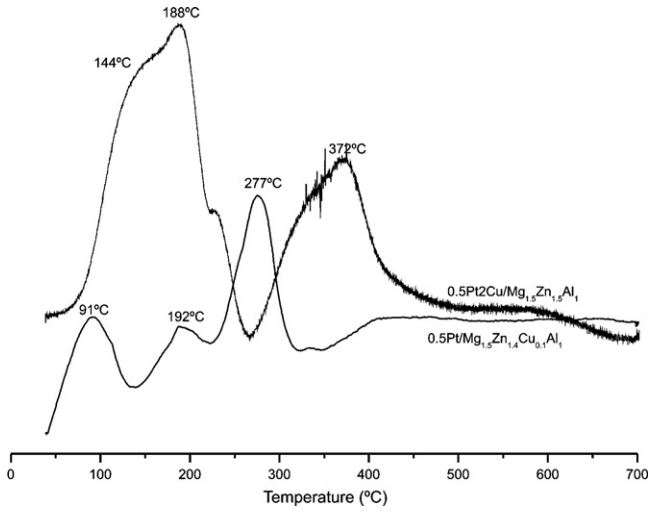

Fig. 7. TPR profiles of (a): 0.5% Pt 2% $Cu/Mg_{1.5}Zn_{1.4}Al_1O$ and (b): 0.5% $Pt/Mg_{1.5}Zn_{1.4}Cu_{0.1}Al_1O$ samples.

co-precipitation in the HT precursor, two Pt-containing catalysts have been prepared. On one hand, 0.5 wt% Pt and 2 wt% Cu were co-impregnated on the $Mg_{1.5}Zn_{1.4}Al_1O$ mixed oxide (0.5% Pt 2% $Cu/Mg_{1.5}Zn_{1.4}Al_1O$) and, on the other hand, 0.5 wt% Pt was impregnated on the $Mg_{1.5}Zn_{1.4}Cu_{0.1}Al_1O$ mixed oxide (0.5% $Pt/Mg_{1.5}Zn_{1.4}Cu_{0.1}Al_1O$). Fig. 7 shows the TPR profiles of both samples. When co-impregnation of the metals is performed in 0.5% Pt 2% $Cu/Mg_{1.5}Zn_{1.4}Al_1O$ two broad and intense peaks at ca. 190 °C and 370 °C are observed. The peak at high temperature is assigned to the reduction of CuO particles, and that at low temperature to the reduction of Pt and Cu sites in close contact.

Due to the broadness of this peak and to the presence of several shoulders, differently interacting Pt and Cu particles are probably present. Higher reducibility is observed for 0.5% $Pt/Mg_{1.5}Zn_{1.4}Cu_{0.1}Al_1O$ with three main peaks at 91, 192 and 277 °C respectively assigned to the reduction of isolated PtO particles, PtO and CuO in close interaction and finally CuO segregated from the mixed oxide support but in strong interaction with it.

3.1.2. Used catalysts

The XRD profiles of some used catalysts obtained following the CPt protocol are reported in Fig. 8. In addition to the peaks assigned to ZnO and Mg(Al)O phases present in the catalyst before reaction, a peak at ca. $2\Theta = 10.6°$ corresponding to the 0 0 3 reflection of a HT phase is also observed in all samples. This is due to the partial reconstruction of the mixed oxides supports in the aqueous media in presence of nitrates owing to their memory effect as previously observed in this process [13,24]. As the memory effect depends on the nature of the cations involved and of the easiness of rehydroxilation of their oxides, the reconstruction is low for the samples of this study due to their high Zn content. It is worthy to note that the crystallinity of the different phases and particularly that the amount of reconstructed HT phase, are improved after reaction in the semi-batch reactor performed during 400 min comparatively to the continuous flow reactor. This accounted for the longer time experiment of the catalyst in the former process.

Catalytic samples were also characterized by FTIR (Fig. 9). The spectra, recorded in the 800–2000 cm^{-1} range show weak bands at 1640, and 1452 cm^{-1} and a more intense band at 1350 cm^{-1}. This latter is assigned to the asymmetric stretching N–O vibration of the NO_3^- [13,25]. These NO_3^- are resent after reconstruction of the

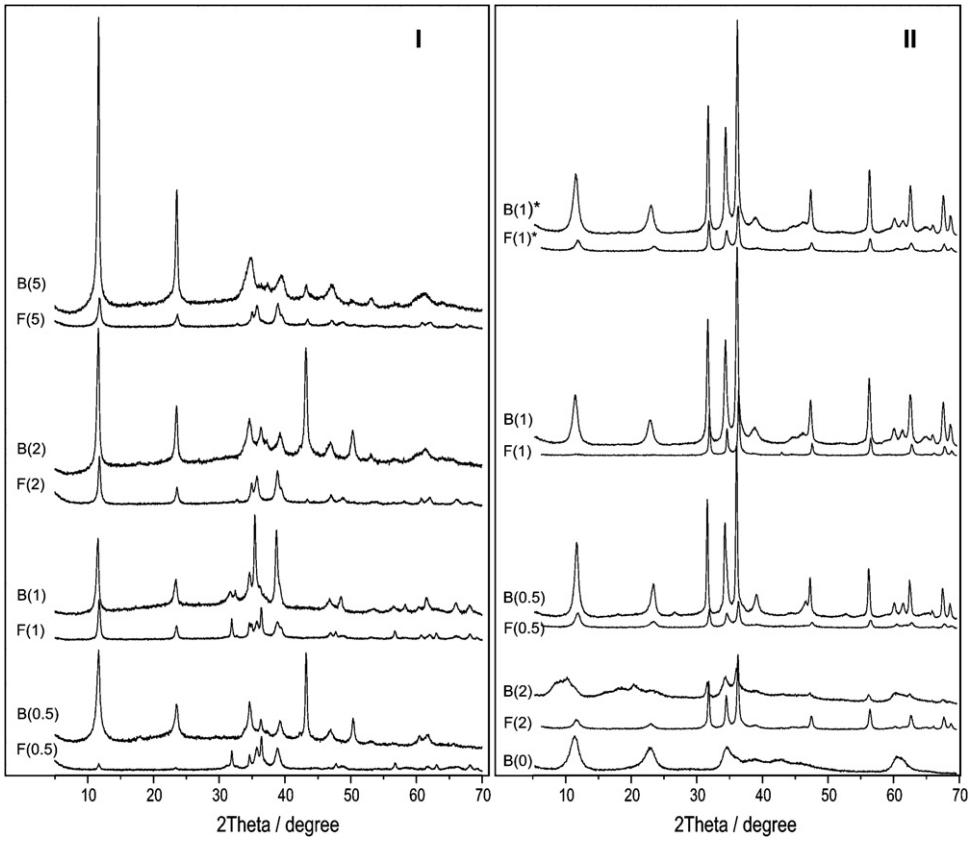

Fig. 8. XRD profiles of used catalysts prepared following the CPt protocol [F: fixed-bed reactor; B: batch reactor; (*X*): Mg/Zn ratio] I: 0.5% Pt/MgZnCuAl; II: 0.5% Pt 2% Cu/MgZnAl(*0.5% $Pt/Mg_{1.5}Zn_{1.4}Cu_{0.1}Al_1$).

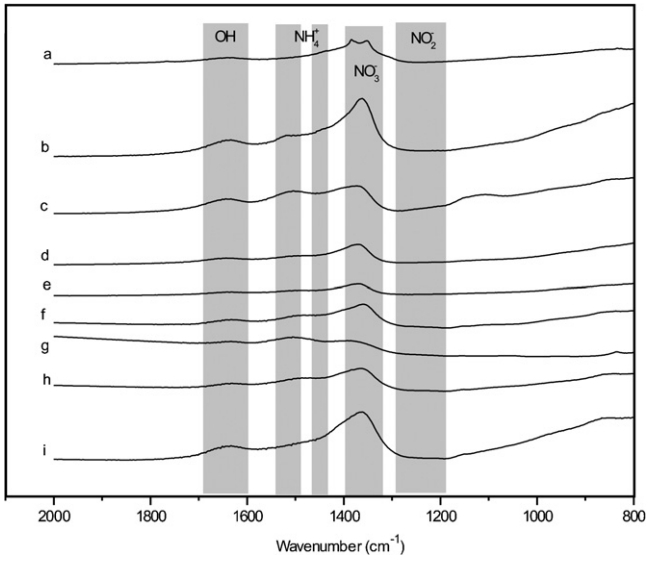

Fig. 9. FTIR spectra of used catalysts at the nitrate reduction process in batch reactor. (a) 0.5% Pt 2% Cu/Mg_2Al_1O; (b): 0.5% Pt 2% Cu/$Mg_2Zn_1Al_1O$; (c): 0.5% Pt 2% Cu/$Mg_1Zn_2Al_1O$; (d): 0.5% Pt 2% Cu/$Mg_{1.5}Zn_{1.5}Al_1O$, (e): 0.5% Pt/$Mg_{1.5}Zn_{1.4}Cu_{0.1}Al_1O$, (f): 0.5% Pt/$Mg_1Zn_1Cu_1Al_1O$; (g): 0.5% Pt/$Mg_{0.5}Zn_1Cu_{1.5}Al_1O$; (h): 0.5% Pt/$Mg_1Zn_{0.5}Cu_{1.5}Al_1O$ and (i): 0.5% Pt/$Mg_{1.5}Zn_{0.3}Cu_{1.2}Al_1O$.

catalysts during reaction, also observed by XRD, with nitrates acting as main compensating anions. The band at 1640 cm^{-1}, assigned to the bending O–H vibration of the water molecules in the interlayer space confirms the reconstruction of the samples. Ammonia is also detected in all samples, except 0.5% Pt/Mg_2Al_1O (spectra a) and 0.5% Pt/$Mg_{1.5}Zn_{0.3}Cu_{1.2}Al_1O$ (spectra i). Regarding the series of 0.5% Pt/$Mg_xZn_yCu_zAl_1O$ samples (spectra f–i) it is noteworthy that the intensity of the band at 1350 cm^{-1} related to the NO_3^- anions increases with the Mg/Zn molar ratio. This is in agreement with the increase of reconstruction degree of the samples.

3.2. Catalytic activity

3.2.1. Batch reactor tests

Catalytic activity results using the batch reactor are shown in Table 1 and in Figs. 10 and 11.

Previous studies [13,24] described the hydrogenation reduction of nitrates as a process with several steps; nitrates were first adsorbed on the mixed oxide surface and also intercalated by anionic exchange between the layers when reconstruction occurs. Then they are reduced by the metals sites (Pt, Pd–Cu, Sn) to nitrites, which are in turn reduced to nitrogen or ammonium. Since the first reduction step did not change the charge of the species, the generated nitrites should remain adsorbed and intercalated in the interlayer space to compensate the positive charges on the layers [26]. However, some nitrites were released into water as a product.

Table 1
Catalytic activity of catalysts (0.5% Pt) by CPt protocol in batch reactor.

Catalyst		Conversion	Selectivity			Yield
Mq/Zn	Composition	$X_{NO_3^-}$	$S_{NO_2^-}$	$S_{NH_4^+}$	S_{N_2}	Y_{N_2}
0.5	$Mg_{0.5}Zn_1Cu_{1.5}Al_1$	97%	0%	55%	45%	44%
1	$Mg_{1.5}Zn_{0.5}Cu_1Al_1$	58%	21%	29%	49%	29%
2	$Mg_1Zn_{0.5}Cu_{1.5}Al_1$	72%	17%	60%	23%	17%
5	$Mg_{1.5}Zn_{0.3}Cu_{1.2}Al_1$	89%	8%	62%	30%	26%
1	$Mg_{1.5}Zn_{1.4}Cu_{0.1}Al_1$	23%	4%	1%	95%	22%
1	$Mg_{1.5}Zn_{1.5}Al_1$ (+2% Cu)	34%	64%	5%	31%	11%
0.5	$Mg_1Zn_2Al_1$ (+2% Cu)	40%	5%	2%	93%	37%
2	$Mg_2Zn_1Al_1$ (+2% Cu)	3%	10%	8%	81%	3%
0	Mg_2Al_1 (+2% Cu)	10%	4%	3%	93%	9%

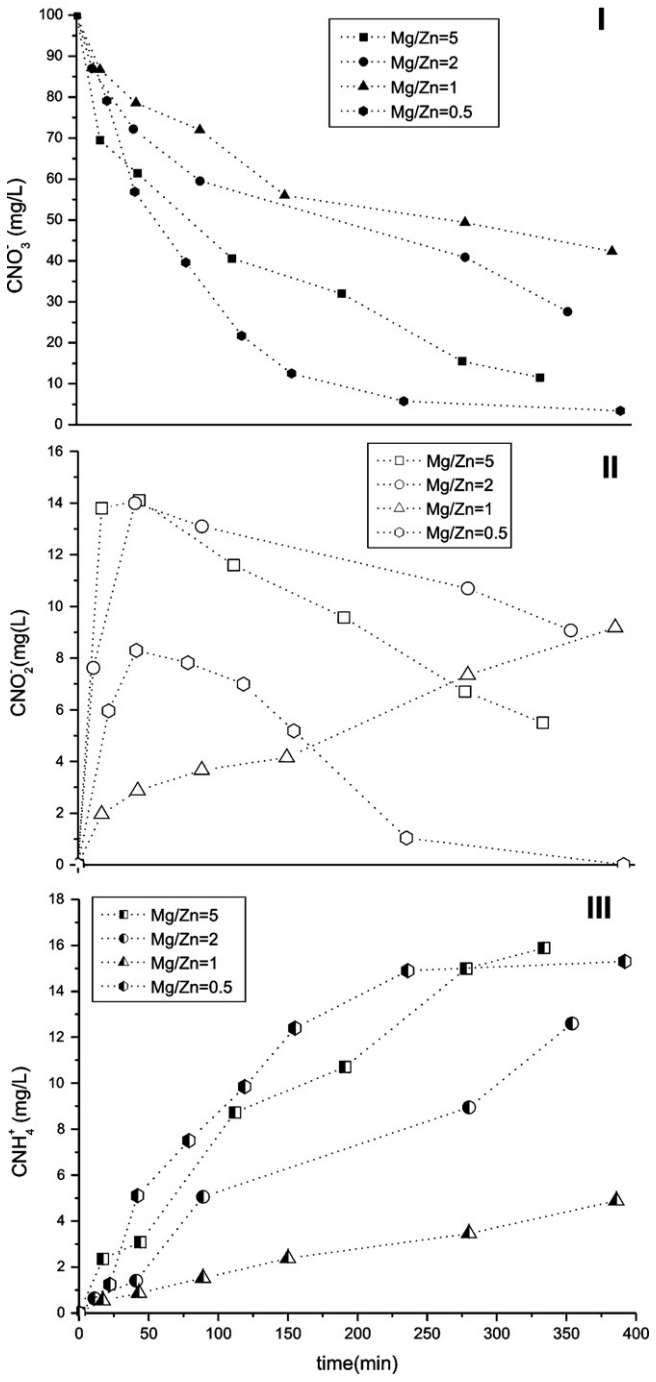

Fig. 10. Concentration profiles in the catalytic reduction of nitrates reaction in batch reactor using 0.5% Pt/MgZnCuAl catalysts obtained following the CPt protocol. I: nitrates; II: nitrites and III: ammonia.

This effect could explain the increase of nitrites formation at the first times of reaction observed in Fig. 10.

The reduction of nitrates compulsorily induced also the release of OH^-, then an increase of pH in the reaction media. It was suggested that on classical non-lamellar supports the resulting basic pH decreases the NO_3^- and NO_2^- adsorption and induces a decrease of reactivity and of selectivity in nitrogen [1]. This was confirmed with monometallic Pd/SiO_2 catalyst using formic acid as reducing agent instead of H_2 [27]. In the case of mixed oxide supports obtained from HT precursors, were the anionic species, i.e. NO_3^-, NO_2^- and OH^-, can be intercalated in the reconstructed catalyst, not only the basicity but also the reconstruction ability of

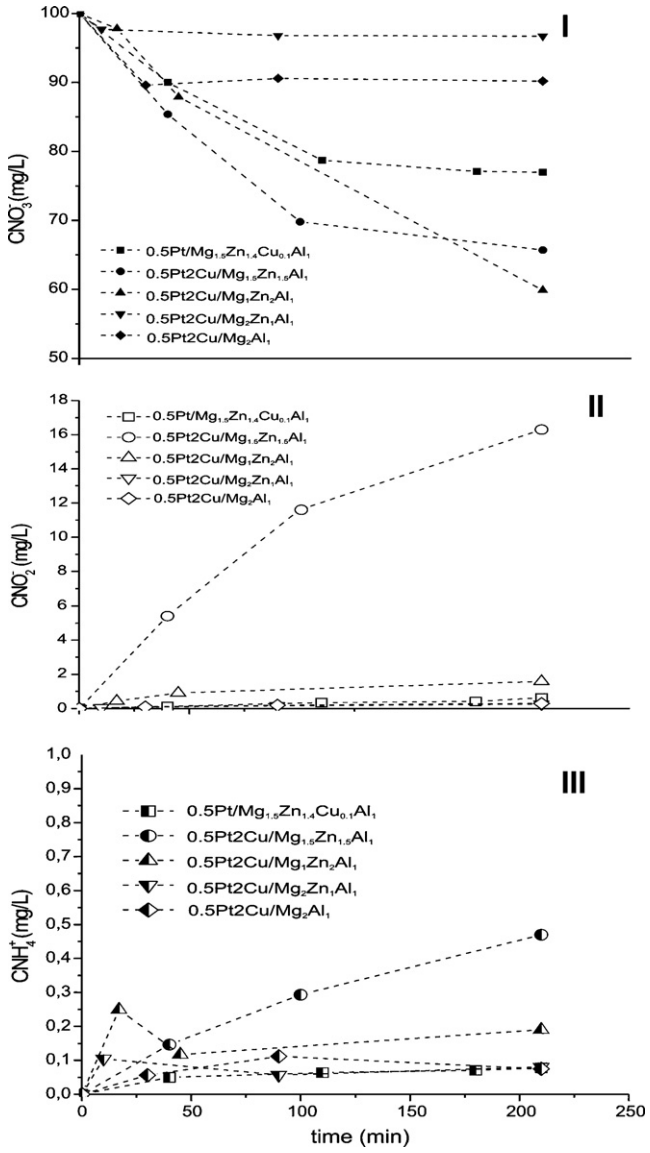

Fig. 11. Concentration profiles in the catalytic reduction of nitrates reaction in batch reactor using 0.5% Pt 2% Cu/MgZnAl catalysts obtained following the CPt protocol. I: nitrates; II: nitrites and III: ammonia.

the samples must determine the activity and selectivity. Palomares et al. [13] suggest that the advantage of the lamellar structure is to diminish the problems of diffusional limitations affecting the selectivity. Regarding the 0.5% Pt/$Mg_xZn_yCu_zAl_1O$ catalysts the basicity and the reconstruction ability are both depending on the Mg/Zn molar ratio. This led us to examine the influence of this parameter on the catalytic properties. Beside the influence of the Cu incorporation protocol which determines the metallic function was also studied.

3.2.1.1. Influence of Mg/Zn ratio. The 0.5% Pt/$Mg_xZn_yCu_zAl_1O$ catalysts obtained following the CPt protocol and with similar Cu molar fraction show high activities ranging from 58 to 97% with selectivity toward nitrogen ranging from 25 to 50%. However, selectivity toward undesired ammonia is high (29 to 62%). It is noteworthy that the higher nitrate conversion is reached with the two samples exhibiting the higher (0.5% Pt/$Mg_{1.5}Zn_{0.3}Cu_{1.2}Al_1O$) and the lower (0.5% Pt/$Mg_{0.5}Zn_1Cu_{1.5}Al_1O$) Mg/Zn molar ratio. Remarkably, 0.5% Pt/$Mg_1Zn_1Cu_1Al_1O$ is the less active catalyst with a conversion of 58%, but gives the higher nitrogen selectivity (49%) and the lower ammonia one (29%). We can assume that there is a straightforward correlation between the Lewis-type basicity of the mixed oxides and the Brønsted-type basicity of the reconstructed HTs. Then the behaviour of the catalysts can be related to the basicity already characterized by the catalytic test of conversion of MBOH showing that the basicity increases with the Mg/Zn molar ratio. On the other hand, the XRD patterns of the used catalysts have shown that the reconstruction ability of the mixed oxides also increases with the Mg/Zn molar ratio. Based on the mechanism previously proposed for the reduction of nitrates with HT catalysts, basicity and reconstruction ability might influence in opposite way the activity and the selectivity to nitrogen. This means that the best compromise is reached in the case of 0.5% Pt/$Mg_1Zn_1Cu_1Al_1O$ with a Mg/Zn molar ratio of 1. 0.5% Pt/$Mg_{1.5}Zn_{0.3}Cu_{1.2}Al_1O$ (Mg/Zn = 5) is strongly active, but due to its high basicity the intercalation of a large amount of OH^- in the highly reconstructed HT structure leads to a high selectivity into NH_4^+ released to the solution and not reduced to nitrogen. 0.5% Pt/$Mg_{0.5}Zn_1Cu_{1.5}Al_1O$ (Mg/Zn = 0.5) whose reconstruction is kinetically limited, is poorly basic and very active, but gives high NH_4^+ selectivity due to diffusional limitations. It must be underline that, except for 0.5% Pt/$Mg_1Zn_1Cu_1Al_1O$, the nitrite formation goes through a maximum at about 1 h of reaction time and the initial rate of formation increases with the Mg/Zn molar ratio of the samples (Fig. 10). This is in agreement with a release of nitrite in solution following the rate of reconstruction and the basicity of the samples which both increase with the Mg content of the catalysts. 0.5% Pt/$Mg_1Zn_1Cu_1Al_1O$ shows a different behaviour with a continuous increase of nitrite formation accounting for the optimum of basicity and reconstruction ability previously reported.

3.2.1.2. Influence of Cu incorporation protocol. The influence of the Cu protocol incorporation has been assessed comparing the activity of the 0.5% Pt 2% Cu/$Mg_{1.5}Zn_{1.5}Al_1O$ and 0.5% Pt/$Mg_{1.5}Zn_{1.4}Cu_{0.1}Al_1O$ catalysts. They contain 2 wt% Cu, therefore the Pt and Cu contents are closer than in the samples of the previous series with about 30 wt% Cu.

Conversion of nitrates reaches 23 and 34% with 0.5% Pt/$Mg_{1.5}Zn_{1.4}Cu_{0.1}Al_1O$ and 0.5% Pt 2% Cu/$Mg_{1.5}Zn_{1.4}Al_1O$, respectively, while selectivity toward nitrites is dramatically higher with this latter sample where it reaches 64%, instead of 4% for the former. The higher activity of the catalyst obtained by impregnation of both Pt and Cu could be related to a better proximity of the metallic sites as suggested by the TPR peak observed below 300 °C (Fig. 7) and assigned to differently interacting Pt and Cu particles. Although, isolated copper cluster surface zones could be coexisting on the surface, responsible of the presence of nitrite. When nitrate is reduced on this zones to nitrites, it cannot reach noble metal surface for further reduction to nitrogen. In this way, the main reason for the high selectivity to nitrite could be not homogeneous surface metal dispersion of Pt and Cu. This leads to low selectivity to nitrogen, in comparison with the Pt/$Mg_{1.5}Zn_{1.4}Cu_{0.1}Al_1$ sample giving 95% of selectivity toward N_2. When copper is co-precipitated during the HT synthesis, it is well dispersed leading to higher selectivity into nitrogen in agreement with previous works [28].

On the other side, if catalytic behaviour of 0.5% Pt 2% Cu/$Mg_{1.5}Zn_{1.5}Al_1O$ and 0.5% Pt 2% Cu/$Mg_1Zn_2Al_1O$ is compared, increase in the Zn molar fraction in the sample improves slightly the nitrate reduction but more significantly the nitrogen yield. This is in agreement with the decrease of basicity of the sample at higher Zn content known to improve the selectivity to nitrogen.

3.2.2. Fixed-bed reactor tests

The activity and selectivity of the 0.5% Pt/$Mg_xZn_yCu_zAl_1O$ catalysts for the hydrogenation of nitrates using a continuous reactor are shown in Table 2.

Table 2
Catalytic activity of 0.5% Pt/$Mg_xZn_yCu_zAl_1O$ catalysts obtained by CPt and CRPt methods using a continuous reactor.

Catalyst		Pt protocol	Conversion	Selectivity		
Mg/Zn	Composition	CPt/CRPt	$X_{NO_3^-}$	$S_{NO_2^-}$	$S_{NH_4^+}$	S_{N_2}
0.5	$Mg_{0.5}Zn_1Cu_{1.5}Al_1$	CPt CRPt	16% 27%	59%77%	22% 5%	19%18%
1	$Mg_1Zn_1Cu_1Al_1$	CPt CRPt	20% 60%	24%38%	0% 1%	76%61%
2	$Mg_1Zn_{0.5}Cu_{1.5}Al_1$	CPt CRPt	17% 25%	25%21%	26%12%	49%67%
5	$Mg_{1.5}Zn_{0.3}Cu_{1.2}Al_1$	CPt CRPt	23% 40%	43%44%	12% 5%	45%51%

All the catalysts present activity in the reduction of nitrates leading to nitrogen and to the undesired nitrites and ammonia. The samples have a same Pt content (0.5 wt%) and a close Cu content of 30 wt%. High nitrite yields are reached. Nitrites are produced on the copper surface and then reduced on Pt. This reaction is highly efficient when the platinum particles are nearby the copper surface or interacting with it. However, due to the high copper loading of the catalysts in comparison with noble metal nitrite produced on the large Cu particles could not be reduced by the noble metal. Moreover, the copper surface oxidized during the reaction cannot be regenerated by the chemisorbed hydrogen from the noble metal, leading to a deactivation of the catalysts.

The results reported in Table 2 also allow evaluating the influence of the basicity of the catalysts on the selectivity at similar nitrate conversion (16–23%), considering the samples obtained following the CPt protocol. Same behaviour observed before in batch reactor configuration is obtained with continuous flow reactor, less basic sample leads to higher selectivity to nitrogen. Also in this case the sample with Mg/Zn = 1 is the most selective than Mg/Zn = 0.5 as was observed before.

The influence of the Cu protocol incorporation has also been assessed comparing the activity of the 0.5% Pt 2% Cu/$Mg_{1.5}Zn_{1.5}Al_1O$ and 0.5% Pt/$Mg_{1.5}Zn_{1.4}Cu_{0.1}Al_1O$ catalysts in the continuous reactor.

In this case, also higher activity is reached when the active metals are co-impregnated on the calcined HT, with larger nitrite presence. Although in this case the nitrite amount is not so high as in the batch reactor. It could be related with the different degree of hydrotalcite reconstruction in the continuous reactor. In terms of ammonia formation, similar behaviour is obtained in comparison with batch reactor results.

3.2.2.1. 0.5% Pt/$Mg_xZn_yCu_zAl_1O$ catalysts: Pt state effects. Close nitrite yields are obtained whatever the protocol used for Pt introduction (CPt or CRPt). In contrast the CRPt and the CPt protocols lead respectively to the higher yields into nitrogen and ammonia. Close contact between the metals favours the nitrate reduction in contrast to alloy formation. Sá and Yoshinaga [6,17] showed that the presence of alloy has a detrimental effect in the selectivity toward nitrogen. This is related with a dilution of noble metal during the alloying which leads to isolated noble metal sites, active for ammonia formation. Therefore the previous results suggest that alloying likely occurs in the case of the CPt protocol.

4. Discussion

Catalytic reduction of nitrates is an extended studied process keeping the drawback of ammonia formation. Previously [16,29] was demonstrated that the acidification of the environment around the active sites improves the selectivity toward nitrogen. On the other hand, hydrotalcite-derived materials have been proved to be adequate catalysts for nitrate reduction, related with adsorptive capacity of these materials, reduced diffusional problems and control OH formation [13,26,28]. Keeping in mind these two ideas, MgZnCuAl hydrotalcite-like materials have been prepared in order to control the acidic properties and introduce the active Cu phase.

Acid–base properties have been evaluated using the catalytic test reaction of conversion of MBOH. It shows that an increase of the Mg contain in the HT, increases the basicity of the mixed oxides. The catalytic reduction of nitrate showed that the higher selectivity to nitrogen is reached with the catalysts of moderate basicity. This is agreement with previous works showing that changing the acid properties of the supports could performed a pH control during the reaction without adding buffers. In this case could be related with two pH control way, first by the hydrotalcite controlling OH– [13,28] and second by the acidity of the support [16].

Previous studies using hydrotalcite-derived materials as catalysts for nitrate reduction were only performed in batch configuration reactor [13,28,30], in this way this work studied also the influence of the reactor configuration with the test of the catalysts in both reactors batch and continuous. Higher activities were obtained in semi-batch than in fixed-bed reactor. It could be generally related with pressure drop, diffusion effects inside the catalyst bed and mainly lower residence time in continuous flow reactor. In this case, it could be also related with the NO_3^- adsorption capacity of the hydrotalcites due to the memory effect. Results showed that the reconstruction occurs mainly in batch reactor than in continuous one, in this way, higher adsorption of nitrates is done. XRD patterns indeed reveal (Fig. 8(I)) the higher reconstruction degree of the catalysts tested in batch reactor comparatively to the fixed-bed reactor. Also, infrared studies show this effect, correlating higher adsorption nitrate capacity with higher catalytic activity as is observed with the sample 0.5% Pt 2% Cu/$Mg_1Zn_2Al_1O$. This sample present bigger peak related with NO_3^- in infrared spectra (Fig. 9), higher reconstruction degree observed by XRD (Fig. 8) and better catalytic performance in the nitrate reaction (Table 1), in comparison with the sample with the sample amount of copper.

The selectivity is also modified. Higher nitrite yields are obtained in fixed-bed reactor in comparison with the batch (see Tables 1 and 3). It is mainly related with this reconstruction ability of this type of catalysts obtained from HT precursors. In batch reactor, accumulation of the intermediates nitrites leads to higher production of ammonia than in fixed-bed reactor (Table 3), in agreement with previous works [31]. Although, in batch reactor higher hydrogen flow was used and the different hydrogen amount during the reaction also affect the ammonia production [32]. From IR study of the used catalysts in batch reactor, mainly no adsorption of NO_2^- is observed, whereas great amount of ammonia adsorbed in the material is detected, This could meant that the intermediate nitrite is released to the solution and then reduced to nitrogen or hydrogenated to ammonia, in agreement with previous mechanism studies with hydrotalcite-derived catalyst for this process [13,24] This is also in agreement with the catalytic data obtained, showing

Table 3
Catalytic activity of 0.5% Pt 2% Cu/$Mg_{1.5}Zn_{1.5}Al_1O$ and 0.5% Pt/$Mg_{1.5}Zn_{1.4}Cu_{0.1}Al_1O$ samples using a continuous reactor.

Catalyst		Conversion	Selectivity			Yield
Mg/Zn	Composition	$X_{NO_3^-}$	$S_{NO_2^-}$	$S_{NH_4^+}$	S_{N_2}	Y_{N_2}
1	$Mg_{1.5}Zn_{1.4}Cu_{0.1}Al_1$	38%	17%	7%	76%	29%
1	$Mg_{1.5}Zn_{1.5}Al_1$ (+2% Cu)	55%	28%		72%	40%

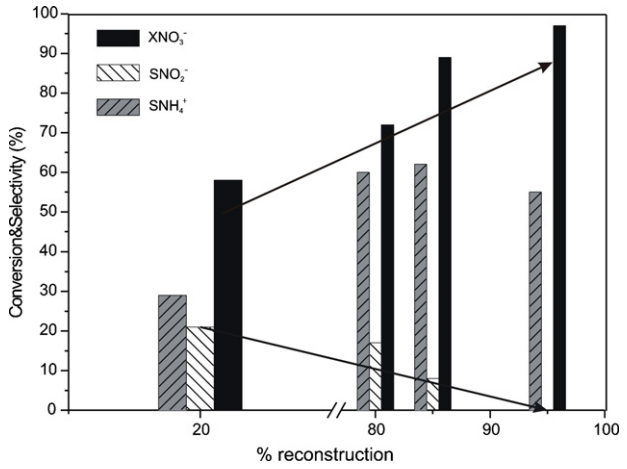

Fig. 12. LDH reconstruction degree related with catalytic results ($X_{NO_3^-}$: nitrate conversion; $S_{NO_2^-}$: nitrite selectivity and $S_{NH_4^+}$ ammonia selectivity).

high selectivity to ammonia and decreasing the nitrite presence with the reaction time.

In order to evaluate the influence of the reconstruction on the catalytic performance of the materials, their reconstruction degree has been evaluated by the integration of the XRD peaks corresponding to the 0 0 3 reflection of the HT phase in the catalyst used in the batch experiment. With this information together with catalytic data, it is observed that in batch reactor higher reconstruction degree in comparison with fixed-bed reactor is obtained. Fig. 12 shows the relationship between the percentage of reconstruction obtained by XRD respect the nitrate conversion ($X_{NO_3^-}$) on one hand, and nitrite ($S_{NO_2^-}$) and ammonia ($S_{NH_4^+}$) selectivity on the other hand. Clear tendencies with an increase in the reconstruction are observed, leading to an increase in the nitrate conversion and a decrease of nitrite formation.

5. Conclusions

The present work clearly shows the influence of the acid–base properties of the catalysts, reactor configuration and reconstruction degree using hydrotalcite-derived catalysts. Incorporation of Zn in the structure leads to a decrease in the basicity of the material leading to a better pH control during the reaction, this effect together with the OH^- control by the hydrotalcite materials results in an increase in selectivity toward nitrogen, the desired product. In this way, based on previous works using hydrotalcites, this system have been optimized in the sense of basicity and noble metal. Also, has been showed how the reconstruction degree is a value parameter for the activity and selectivity optimization, with a direct dependence with the reactor configuration employed.

Additional studies involving the development of realistic kinetic models, including catalyst deactivation and product distribution evolution, are being performed in both types of reactors, in order to clarify and quantify the effect of the catalyst composition (Mg/Zn ratio, Pt and Cu content, impregnation protocol method, etc.), over the catalyst stability and selectivity.

Acknowledgements

This work was financial supported by the CTP (Project 2008ITT-CTP-00111, and CTPP02/08) by the Spanish Ministry of Science and Innovation (Project CTQ2007-62545/PPQ).

References

[1] K.D. Vorlop, T. Tacke, Chemie Ingenieur Technik 61 (1989) 836.
[2] J. Wärnå, I. Turunen, T. Salmi, T. Maunula, Chemical Engineering Science 49 (1994) 5763.
[3] F. Epron, F. Gauthard, C. Pineda, J. Barbier, Journal of Catalysis 198 (2001) 309.
[4] A. Pintar, J. Batista, J. Levec, T. Kajiuchi, Applied Catalysis B: Environmental 11 (1996) 81.
[5] A. Pintar, J. Batista, Catalysis Today 53 (1999) 35.
[6] J. Sa, H. Vinek, Applied Catalysis B: Environmental 57 (2005) 247.
[7] J. Sa, D. Gasparovicova, K. Hayek, E. Halwax, J.A. Anderson, H. Vinek, Catalysis Letters 105 (2005) 209.
[8] Z.Y. Xu, L.Q. Chen, Y. Shao, D.Q. Yin, S.R. Zheng, Industrial & Engineering Chemistry Research 48 (2009) 8356.
[9] K. Nakamura, Y. Yoshida, I. Mikami, T. Okuhara, Applied Catalysis B: Environmental 65 (2006) 31.
[10] D. Gasparovicova, M. Kralik, M. Hronec, Z. Vallusova, H. Vinek, B. Corain, Journal of Molecular Catalysis A: Chemical 264 (2007) 93.
[11] A. Garron, K. Lazar, F. Epron, Applied Catalysis B: Environmental 59 (2005) 57.
[12] N. Barrabes, J. Just, A. Dafinov, F. Medina, J.L.G. Fierro, J.E. Sueiras, P. Salagre, Y. Cesteros, Applied Catalysis B: Environmental 62 (2006) 77.
[13] A.E. Palomares, J.G. Prato, F. Rey, A. Corma, Journal of Catalysis 221 (2004) 62.
[14] X.M. Xie, J.X. Liu, J.L. Song, Z.Z. Wang, Chinese Journal of Catalysis 24 (2003) 569.
[15] Y. Wang, J.H. Qu, H.J. Liu, Journal of Molecular Catalysis A: Chemical 272 (2007) 31.
[16] N. Barrabes, A. Dafinov, F. Medina, J.E. Sueiras, Catalysis Today 149 (2010) 341.
[17] Y. Yoshinaga, T. Akita, I. Mikami, T. Okuhara, Journal of Catalysis 207 (2002) 37.
[18] U. Costantino, F. Marmottini, M. Sisani, T. Montanari, G. Ramis, G. Busca, M. Turco, G. Bagnasco, Solid State Ionics 176 (2005) 2917.
[19] I. Atake, K. Nishida, D. Li, T. Shishido, Y. Oumi, T. Sano, K. Takehira, Journal of Molecular Catalysis A: Chemical 275 (2007) 130.
[20] V.Y. Irkhin, M.I. Katsnelson, A.V. Trefilov, Europhysics Letters 15 (1991) 649.
[21] K. Nishida, D.L. Li, Y.Y. Zhan, T. Shishido, Y. Oumi, T. Sano, K. Takehira, Applied Clay Science 44 (2009) 211.
[22] F. Cavani, F. Trifirò, A. Vaccari, Catalysis Today 11 (1991) 173.
[23] O.S.G.P. Soares, J.J.M. Órfão, J. Ruiz-Martínez, J. Silvestre-Albero, A. Sepúlveda-Escribano, M.F.R. Pereira, Chemical Engineering Journal 165 (2010) 78.
[24] Y. Wang, J.H. Qu, H.J. Liu, C.Z. Hu, Catalysis Today 126 (2007) 476.
[25] S.D. Ebbesen, B.L. Mojet, L. Lefferts, Journal of Catalysis 256 (2008) 15.
[26] D.J. Wan, H.J. Liu, X. Zhao, J.H. Qu, S.H. Xiao, Y.N. Hou, Journal of Colloid and Interface Science 332 (2009) 151.
[27] A. Garron, F. Epron, Water Research 39 (2005) 3073.
[28] Y. Wang, J.H. Qu, H.J. Liu, R.C. Wu, Chinese Science Bulletin 51 (2006) 1431.
[29] D. Gasparovicova, M. Kralik, M. Hronec, Collection of Czechoslovak Chemical Communications 64 (1999) 502.
[30] A.E. Palomares, J.G. Prato, F. Marquez, A. Corma, Applied Catalysis B: Environmental 41 (2003) 3.
[31] M.B. Sell, M.D. Bonse, Vom Wasser 79 (1992) 129.
[32] S.D. Ebbesen, B.L. Mojet, L. Lefferts, Journal of Physical Chemistry C 113 (2009) 2503.